Cellular and Molecular Bioengineering
https://doi.org/10.1007/s12195-023-00774-y

SI: 2023 CMBE YOUNG INNOVATORS

siRNA Lipid–Polymer Nanoparticles Targeting E-Selectin and Cyclophilin A in Bone Marrow for Combination Multiple Myeloma Therapy

Christian G. Figueroa-Espada[1] · Pedro P. G. Guimarães[2] · Rachel S. Riley[3] · Lulu Xue[1] · Karin Wang[4] · Michael J. Mitchell[1,5,6,7,8,9,10]

Received: 20 February 2023 / Accepted: 20 July 2023

Abstract

Introduction Multiple myeloma (MM) is a hematological blood cancer of the bone marrow that remains largely incurable, in part due to its physical interactions with the bone marrow microenvironment. Such interactions enhance the homing, proliferation, and drug resistance of MM cells. Specifically, adhesion receptors and homing factors, E-selectin (ES) and cyclophilin A (CyPA), respectively, expressed by bone marrow endothelial cells enhance MM colonization and dissemination. Thus, silencing of ES and CyPA presents a potential therapeutic strategy to evade MM spreading. However, small molecule inhibition of ES and CyPA expressed by bone marrow endothelial cells remains challenging, and blocking antibodies induce further MM propagation. Therefore, ES and CyPA are promising candidates for inhibition via RNA interference (RNAi).

Methods Here, we utilized a previously developed lipid–polymer nanoparticle for RNAi therapy, that delivers siRNA to the bone marrow perivascular niche. We utilized our platform to co-deliver ES and CyPA siRNAs to prevent MM dissemination in vivo.

Results Lipid-polymer nanoparticles effectively downregulated ES expression in vitro, which decreased MM cell adhesion and migration through endothelial monolayers. Additionally, in vivo delivery of lipid-polymer nanoparticles co-encapsulating ES and CyPA siRNA extended survival in a xenograft mouse model of MM, either alone or in combination with the proteasome inhibitor bortezomib.

Conclusions Our combination siRNA lipid-polymer nanoparticle therapy presents a vascular microenvironment-targeting strategy as a potential paradigm shift for MM therapies, which could be extended to other cancers that colonize the bone marrow.

Keywords RNAi · Blood cancer · Nanomedicine

Introduction

Multiple myeloma (MM) is characterized by an abnormal proliferation and accumulation of malignant plasma cells in the bone marrow [1, 2]. Current U.S. Food and Drug Administration (FDA)-approved MM therapies have shown an increase in disease-free survival and have successfully improved the overall 5-year survival rate to a 55% [3, 4]. For instance, the proteasome inhibitor bortezomib, a therapy for newly diagnosed and relapsed/refractory MM patients, has shown to be effective and well-tolerated with overall response rates over 40% [5]. However, initial remission periods last 2 to 3 years [6, 7], with patients developing resistance to such therapy, and subsequently facing shorter survival times. Thus, there is an urgent clinical need for improved therapies against MM.

Given the complexity of the disease, significant efforts have been made to understand the biology of MM and the implications of the surrounding microenvironment [8–11]. Studies have shown that physical interactions between MM cells and the cellular compartment of the bone marrow niche enable disease progression and drug resistance [12–14]. Therefore, in designing innovative therapies to use in MM patients independent of the genomic complexity of MM cells, an attractive approach could be to target the

Associate Editor Michael R. King oversaw the review of this article.

Extended author information available on the last page of the article

Published online: 14 September 2023

physical interactions between MM cells and the bone marrow microenvironment. Recent studies have shown that bone marrow endothelial cells are major contributors to MM progression (Fig. 1) [15–17]. Specifically, the adhesion receptor constitutively expressed by bone marrow endothelium and responsible for leukocyte recruitment to diseased tissue [18, 19], E-selectin (ES), enables cancer cell rolling and adhesion to the vasculature contributing to subsequent dissemination to distant tissues [17, 20]. Additionally, it had been shown that the homing factor cyclophilin A (CyPA), a receptor with important roles such as T-cell activation [21], is not only expressed but also highly secreted by the bone marrow endothelium in the context of MM, and promotes their colonization, proliferation, and drug resistant abilities of these cancer cells [15]. Thus, inhibition of both ES and CyPA could provide a therapeutic strategy to halt MM progression and evade drug resistance.

Direct and specific inhibition of adhesion receptors and homing factors from bone marrow endothelial cells by small molecules remains challenging. Thus, ES and CyPA are promising candidates for combination RNA interference (RNAi) therapy, which inhibits traditionally undruggable targets by reducing their messenger RNA (mRNA) expression [22, 23]. Small interfering RNA (siRNA) is a valuable tool to treat disease by inhibiting the expression of any targeted protein implicated in disease progression [24, 25]. However, there are two main challenges that hinder the implementation of siRNA therapeutics to treat diseases. First, siRNA is unstable in the bloodstream and is quickly degraded by nucleases [26, 27]. Further, siRNA cannot readily traverse cell membranes without complexation with transfection reagents that are not applicable for in vivo use [28]. Nanoparticle (NP) delivery systems can overcome these obstacles for successful siRNA delivery by protecting the siRNA cargo, preventing degradation, and avoiding renal clearance while enabling cellular uptake [27]. One example of the clinical translation of NPs is the NP-based mRNA vaccines against COVID-19, developed by Moderna and Pfizer/BioNTech [29], which received FDA emergency use authorization in 2020. Therefore, we hypothesized that suppression of ES and CyPA simultaneously from bone marrow endothelium using NPs encapsulating siRNA may decrease MM extravasation and colonization of bone marrow.

In previous work, we utilized high-throughput screening of NPs via molecular barcoding to identify an optimal NP formulation to enable siRNA delivery to bone marrow in vivo [30]. We showed that our NP formulation successfully silenced CyPA (siCyPA-NPs) in bone marrow endothelial cells, which decreased MM cell adhesion and invasion in vitro, and extended survival in a xenograft mouse model of MM. Here, we used our optimal NP formulation to encapsulate ES siRNA for effective ES gene silencing in endothelial cells in vitro, which decreased MM cell adhesion to endothelial monolayers in vitro. Further, we co-encapsulated both ES and CyPA siRNAs for their simultaneous inhibition in bone marrow in vivo, and combined it with bortezomib

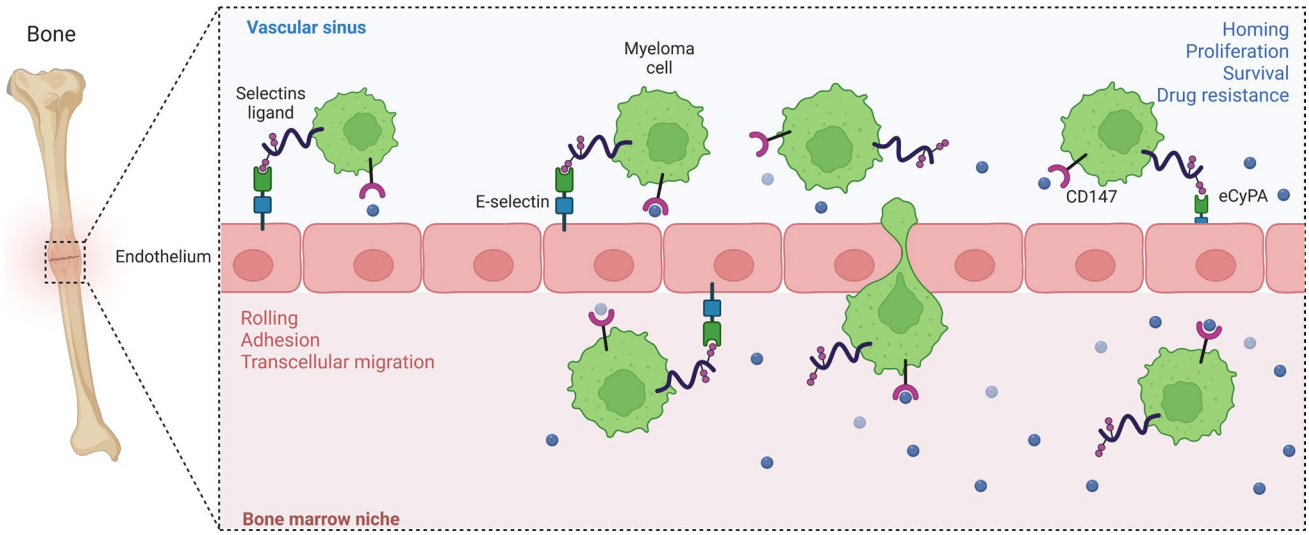

Fig. 1 Adhesion receptors and homing factors expressed by bone marrow endothelial cells promote myeloma cell dissemination and survival. Illustration showing physical interactions between myeloma and bone marrow endothelial cells mediated by the adhesion receptor E-selectin, which binds to selectin ligands expressed on the surface of myeloma cells, and the homing factor, cyclophilin A, through its axis with CD147. E-selectin induces myeloma cell extravasation by (i) rolling and (ii) adhesion of myeloma cells to the vascular lining, and together with cyclophilin A, (iii) their transcellular migration. Cyclophilin A, on the other hand, acts as a chemoattractant promoting the homing, proliferation, survival, and ultimately drug resistance of myeloma cells via the CD147 receptor. Created with BioRender.com

for a synergistic therapeutic effect, which led to extended survival of mice when compared to our previous studies. These data suggest that a vascular microenvironment combination RNAi approach can be utilized as a potential therapeutic strategy for MM, and could potentially be utilized to treat other cancers that colonize the bone marrow.

Results and Discussion

Polymer-Lipid siRNA NP Synthesis and Characterization

We have previously optimized a NP formulation for effective siRNA delivery to bone marrow endothelium using high-throughput screening via molecular barcoding [30]. This formulation consists of a polymer–lipid hybrid material, named 7C1, obtained by Michael addition chemistry synthesizing low-molecular weight polyethylenimine (PEI) and epoxide-terminated lipids as shown in Fig. 2a [31–34]. Following purification of the polymer–lipid hybrid, NPs were formulated by combining an ethanol phase comprised of 7C1, and $C_{18}PEG_{1000}$, at a mole ratio of 70:30, respectively, with an aqueous phase containing the siRNAs via chaotic mixing in a microfluidic device (Fig. 2b). NPs were characterized based on their size, surface charge, and morphology. Dynamic light scattering (DLS) measurements showed that each NP formulation was between 75 and 90 nm in diameter for ES siRNA (siES)-NPs or NPs co-encapsulating CyPA siRNA (siCyPA) and siES, as shown in Fig. 2c,d, and zeta potential (ζ) values were around − 1 mV, with no change observed for either NP formulation (Fig. 2c). Cryogenic-transmission electron microscopy (cryo-TEM) showed that NPs had a multilamellar structure and were monodisperse (Fig. 2e), corroborating results from our previous studies [32, 35].

In Vitro Efficacy of Polymer–Lipid siRNA NPs

We next evaluated the silencing abilities of our NP formulation encapsulating siES on murine endothelial (bEnd.3) cells. Using real-time quantitative reverse transcription polymerase chain reaction (RT-qPCR), we confirmed effective gene knockdown, in a dose-response manner, compared to bEnd.3 monolayers treated with scrambled control siRNA (siControl)-NPs (Fig. 3a). However, to ensure that our NP

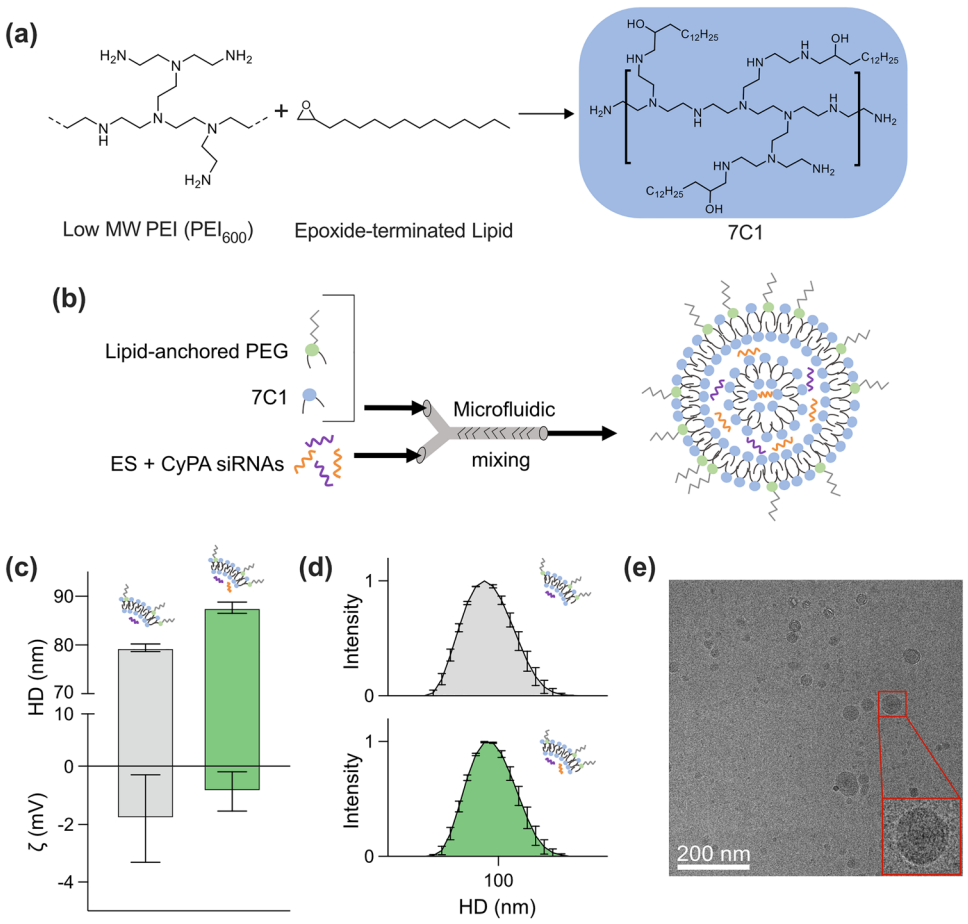

Fig. 2 Synthesis and characterization of nanoparticles (NPs) co-encapsulating E-selectin (ES) and cyclophilin A (CyPA) siRNAs. (**a**) Synthesis of the lipid–polymer hybrid 7C1 through a ring-opening reaction. (**b**) NP formulation diagram demonstrating co-encapsulation of ES and CyPA siRNAs through chaotic mixing in microfluidic devices for in vitro and in vivo studies. (**c**) Hydrodynamic diameter (HD) measured by dynamic light scattering (DLS) and zeta potential (ζ) values for NPs encapsulating ES siRNA or both ES and CyPA siRNAs. n = 3 independent experiments. Error bars indicate standard deviation. (**d**) Comparison of HD against normalized intensity for both NP formulations, siES-NP and siES + siCyPA-NP. n = 3 independent experiments. Error bars indicate standard deviation. (**e**) Cryogenic transmission electron microscopy (cryo-TEM) of siES + siCyPA-NP

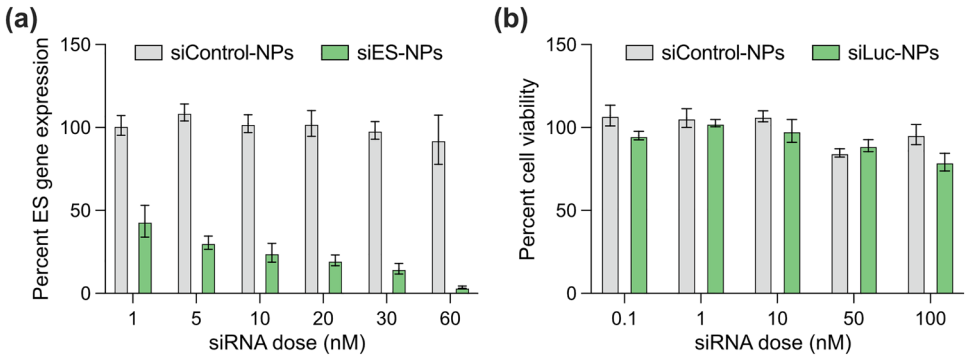

Fig. 3 Gene silencing and cytotoxicity of siES-NPs in vitro. (**a**) ES gene expression from murine endothelial cells (bEnd.3) treated with 1–60 nM of siControl-NPs or siES-NPs for 24 h prior to RT-qPCR analysis. n = 6 independent experiments. Error bars indicate standard deviation. (**b**) HeLa cell viability 24 h after treatment with 1–100 nM of siControl-NPs or siLuc-NPs. n = 3 independent experiments. Error bars indicate standard deviation

formulation delivers siRNA in vitro safely, HeLa cells that stably express firefly and Renilla luciferase were used to evaluate siRNA NP-induced cytotoxic effects. HeLa cells have been widely utilized to evaluate the in vitro efficacy of a variety of NPs due to the cost-effectiveness and simplicity of the assay, as its readout can be obtained using a luminescence microplate reader [31, 36]. Thus, to study cytotoxic effects, luciferase siRNA (siLuc) was encapsulated in the NP formulation (siLuc-NPs) and administered to HeLa cells at concentrations ranging from 0.1 to 100 nM. Both the efficacy and safety of our siLuc-NPs were assessed using luciferase and luminescence-based assays, which revealed that while luciferase expression decreased as a function of siRNA concentration (Fig. S1a), no cytotoxic effects were observed (Fig. 3b). Further, before proceeding to other in vitro studies, we tested whether NP efficacy in delivering siRNA safely was higher than commercially available transfection reagents. Thus, we evaluated, using HeLa cells, how our NP formulation performed in comparison to DharmaFECT, a commonly used transfection reagent for siRNA delivery [37]. We showed that at a siRNA concentration of 10 nM, our lead NP formulation silenced luciferase significantly when compared to the DharmaFECT treatment (Fig. S1b), with no cytotoxic effects observed for either delivery method (Fig. S1c). These data further confirm our NP formulation is efficient and safe for siRNA delivery in vitro.

Treating Endothelial Cells with siES-NPs Disrupts Interactions with MM Cells In Vitro

ES is constitutively expressed on the bone marrow endothelium and allows MM cells to roll, adhere, and migrate through endothelium to reach distant bone marrow sites [17, 20]. Hence, we chose to downregulate ES expression to inhibit MM cell extravasation and evade disease spread. To evaluate the effect that ES silencing has on MM cell transendothelial migration, we conducted transwell assays in a co-culture setting using murine endothelial cells as a model for bone marrow endothelial cells. bEnd.3 monolayers were seeded and activated with TNF-α, followed by treatment with either siControl-NPs or siES-NPs, before the addition of Luc+/GFP+ MM.1S cells. After 24 h, we measured luminescence signal which revealed a 29% lower signal when bEnd.3 monolayers were treated with siES-NPs (Fig. 4a). Further, we assessed how the downregulation of ES impacted the ability of MM cells to adhere to endothelial monolayers. In a similar setting, we co-cultured bEnd.3 cells, either treated with siControl-NPs or siES-NPs, with Luc+/GFP+MM.1S cells, and observed 85.8% less adhesion of MM cells to monolayers when these were treated with siES-NPs (Fig. 4b), which was also demonstrated using confocal microscopy by the number of GFP + cells (Fig. 4c). These results demonstrate that knockdown of ES expressed by endothelial cells hinders the capability of MM cells to adhere and migrate across endothelial monolayers, which we anticipate could hinder MM progression in vivo. Collectively, these data suggest that siES-NPs induce potent gene silencing in endothelial monolayers and significantly reduce MM cell extravasation in vitro, and lay the foundation to evaluate this strategy in vivo.

Co-treatment of siES + siCyPA-NPs and Bortezomib Extends Survival in a Xenograft Mouse Model of MM

Given our previous work where we demonstrated that inhibition of CyPA in combination with bortezomib extended survival in a mouse model of MM [30], and by confirming that downregulation of ES disrupts physical interactions between MM and endothelial cells in vitro, we proceeded to co-encapsulate siES and siCyPA to probe the therapeutic efficacy of our combination RNAi strategy in vivo. To determine overall survival of mice, we injected 2×10^6

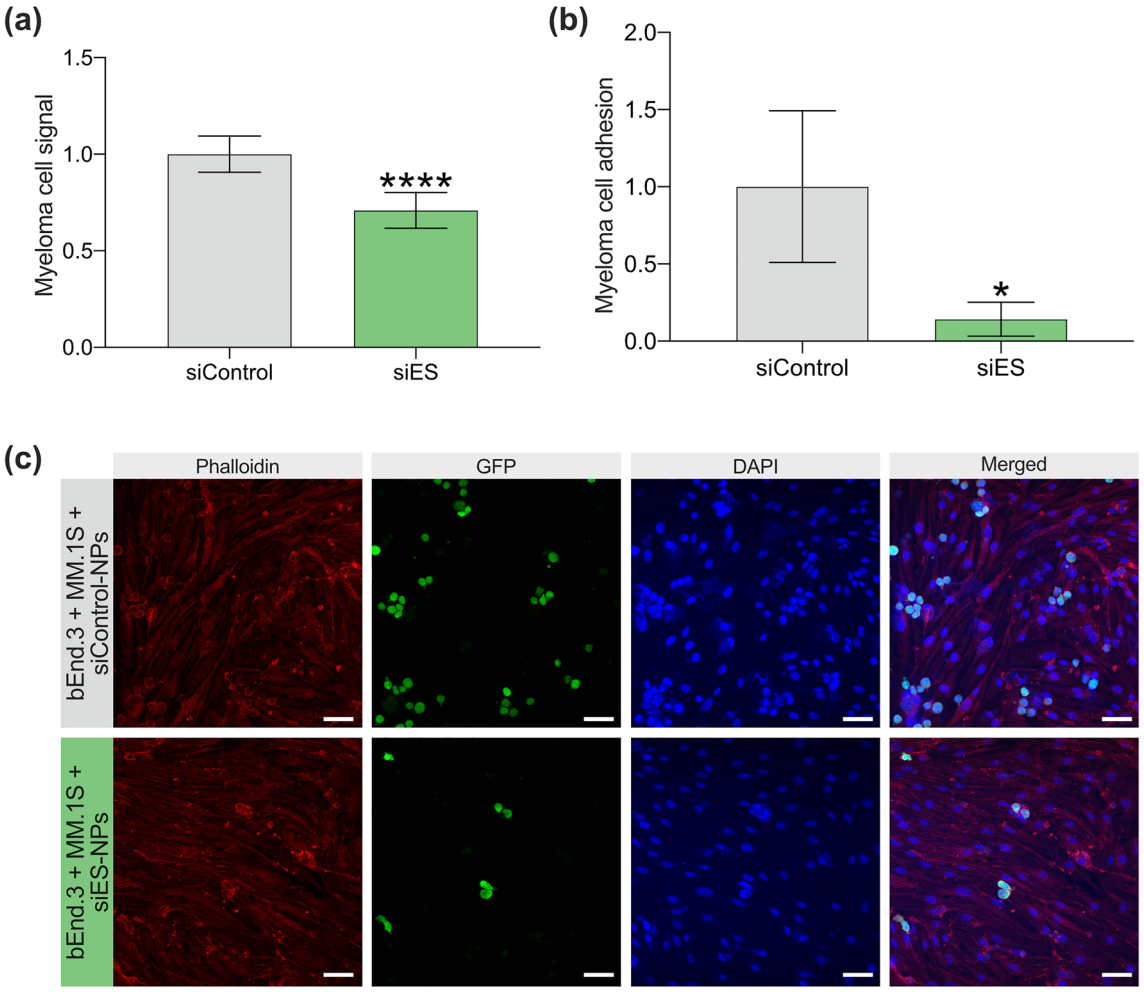

Fig. 4 Disruption of physical interactions between myeloma and endothelial cell monolayers via NP-based siRNA silencing of ES. (**a**) Myeloma cell invasion through monolayers of bEnd.3 cells treated with 60 nM siControl-NPs or siES-NPs. n = 3 independent experiments, ****p < 0.0001. Error bars indicate standard deviation. (**b**) Myeloma cell adhesion to bEnd.3 monolayers treated with 60 nM of siControl-NPs or siES-NPs. n = 4 independent experiments, *p < 0.01. Error bars indicate standard deviation. (**c**) Representative images showing myeloma cell adhesion to bEnd.3 monolayers treated with 60 nM of siControl-NPs or siES-NPs. Scale bars: 50 μm

Luc+/GFP+MM.1S cells via tail vein injection on day 0, and allowed tumors to grow for 30 days prior to treatment (Fig. 5a). On day 30, mice were intravenously injected with 1.0 mg/kg of siES + siCyPA-NPs with or without 0.5 mg/kg of bortezomib. These treatments were repeated twice per week, with NPs being injected intravenously, and bortezomib intraperitoneally. The results showed an extended survival of up to 100 days when mice were treated with siES + siCyPA-NPs and bortezomib combined, compared to 65 days for those treated with siES + siCyPA-NPs or bortezomib alone (Fig. 5b). Notably, our results showed similar survival of mice when treated with bortezomib or siES + siCyPA-NPs, suggesting that downregulation of ES and CyPA is vital to increase the therapeutic effect of bortezomib in vivo. Remarkably, these data indicate targeting the physical interactions that are primarily mediated by ES and CyPA decreases MM spread, which is confirmed by extended survival in a mouse model of MM.

Conclusion

Here we used a previously developed NP formulation by our group [32] for siRNA delivery to inhibit the adhesion molecule and homing factor, ES and CyPA, respectively, in bone marrow for MM therapy in vivo. ES and CyPA have been shown to play key roles in the extravasation, proliferation, survival, and drug resistance of MM [15–17, 20]. Thus, we sought to simultaneously inhibit ES and CyPA expression in bone marrow using NPs in vivo, and assess the effect of this strategy in treating MM. In previous work [30], we demonstrated effective siRNA-NP-based

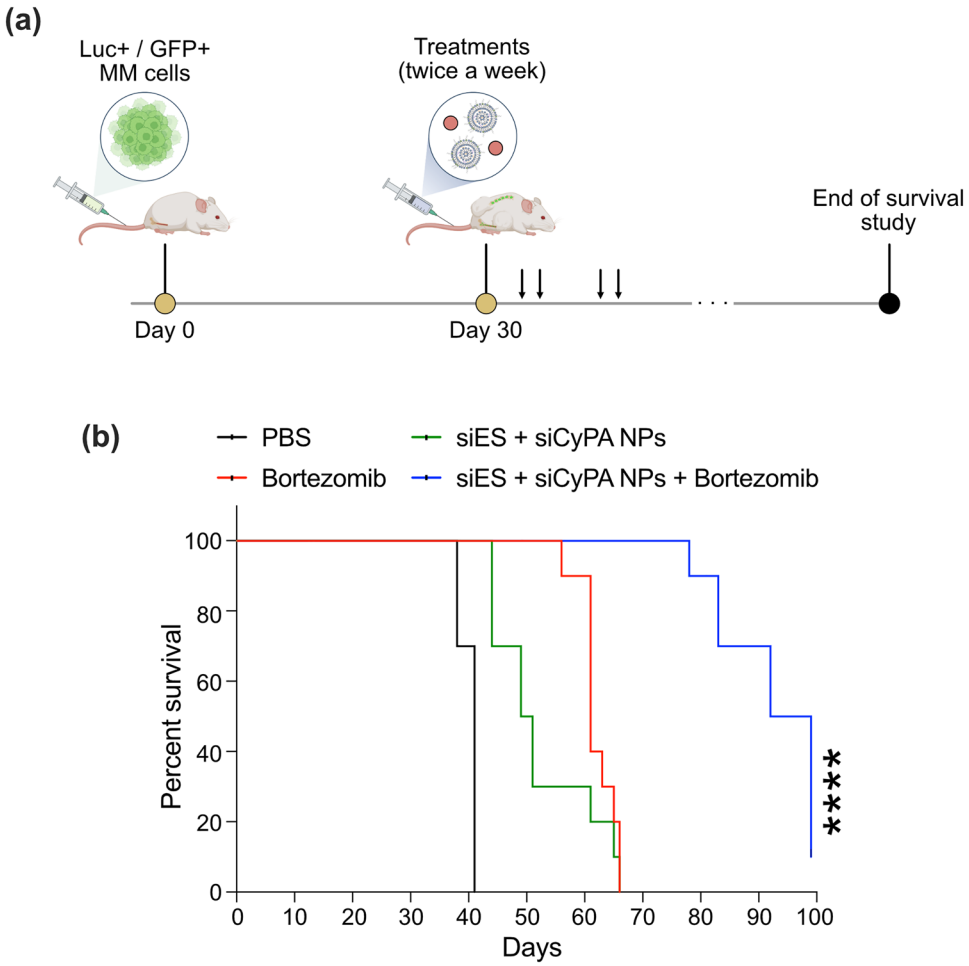

Fig. 5 NP co-delivery of ES and CyPA siRNAs in combination with bortezomib extends overall survival. (**a**) Treatment regimen carried out for the in vivo studies. Mice were injected I.V. with Luc+/GFP+MM.1S on Day 0, and treatment groups (PBS, bortezomib, siES + siCyPA-NPs, or siES + siCyPA-NPs + bortezomib) were injected I.V. or I.P. twice a week on Day 30. (**b**) Survival data of mice with myeloma tumors following treatment groups. n = 10 mice/group, ****$p < 0.0001$ with log-rank test

inhibition of CyPA both in vitro and in vivo, and showed that disrupting the physical interactions between MM cells and bone marrow endothelial cells, mediated by CyPA, decreased the ability of MM cells to invade and adhere to bone marrow endothelium. Moreover, we showed that combining siCyPA-NPs, with or without bortezomib, decreased tumor burden, extended survival of mice, and increased the therapeutic effect of bortezomib in a mouse model of MM. Therefore, in this work, we explored the effects of inhibiting ES expressed by endothelial monolayers in vitro, and found that when ES was downregulated, MM cell adhesion and migration through endothelial monolayers was reduced when compared to the untreated monolayers. Thus, we hypothesized that simultaneous inhibition of ES and CyPA, whose overexpression and secretion, respectively, play a role in MM progression, would provide a strategy to further disrupt interactions between MM cells and the bone marrow endothelium, reducing MM cell dissemination to distant bone marrow sites. Our data confirmed in vivo administration of siES + siCyPA-NPs extended survival of mice similarly to bortezomib-treated mice, and suggested that a combination of siES + siCyPA-NPs with bortezomib created a synergistic effect that sensitized MM cells to bortezomib therapy. Of note, some limitations in our study include the potential side-effects of suppressing ES and CyPA simultaneously in the context of the immune system [38], given their important roles in leukocyte recruitment and T-cell activation, respectively. Future studies are needed to address these potential effects using immunocompetent mice and eventually non-human primates to effectively assess the safety of our siRNA NP strategy. In conclusion, this proof-of-concept study presents a vascular microenvironment combination RNAi therapy for MM, as means to evade its spreading and overcome drug resistance, which can potentially be applied to target other vascular beds within the body to treat other malignancies. Overall, the present work demonstrates the impact of the surrounding bone marrow microenvironment on MM cells, particularly on the adhesion, migration, and spreading of MM cells, and how targeting these interactions between the microenvironment and MM cells using siRNA NP technology is a promising way to treat MM.

Materials and Methods

Polymer–Lipid Synthesis

Polymer–lipids were synthesized by reacting low molecular PEI (Sigma-Aldrich, St. Louis, MO, US) with C15 epoxide terminated alkyl tails (Tokyo Chemical Industry, Tokyo, Japan) at 90 °C in 100% ethanol for 48–72 h at a 14:1 molar ratio as described previously (Fig. 2a) [31]. Polymer–lipids were purified via flash chromatography to separate the optimized hydrophobic C15:hydrophilic PEI ratio, as described previously [31, 32].

Polymer–Lipid NP Formulation

NPs were formed by combining an aqueous phase containing siRNA with an ethanol phase containing the polymer–lipid and a polyethylene glycol (PEG)-lipid conjugate via controlled mixing in a microfluidic device [23]. Specifically, the ethanol phase contained the polymer–lipid (7C1) and a PEG-lipid conjugate (C18), PEG molecular weight (1000 kDa), at a PEG mole percentage of 30% by weight (Avanti Polar Lipids, Alabaster, AL, US) as shown in Fig. 2b. The aqueous phase was prepared in 10 mM citrate, pH 3.0 buffer (Teknova, Hollister, CA, US) with scrambled control siRNA (siControl), ES siRNA (siES), or siES and CyPA siRNAs (siCyPA) (siES + siCyPA). Syringe pumps were used to perfuse the ethanol and aqueous phases at a 2.5:1 ratio through the microfluidic device. The resulting NPs were dialyzed against PBS at room temperature for 2 h and then extruded through a 0.22 µm sterile filter (Genesee Scientific, San Diego, CA, US).

NP Characterization

siRNA concentration and encapsulation in NPs was determined using a NanoDrop Spectrophotometer (Thermo Fisher Scientific, Waltham, MA, US) and a modified Quant-iT RiboGreen RNA assay (Thermo Fisher Scientific), as previously described [35, 39]. NP hydrodynamic diameter and polydispersity (PDI) were measured using a Zetasizer Nano ZS machine (Malvern Panalytical, Malvern, UK). For analysis of NP structure using cryogenic-transmission electron microscopy (cryo-TEM), NPs samples were prepared in a vitrification system (25 °C, ~ 100% humidity). Briefly, 3 µL sample of NP solution was dropped on a lacey copper grid coated with a continuous carbon film and blotted to remove excess sample without damaging the carbon layer. A grid was mounted on a Gatan 626 single tilt cryogenic holder equipped in the TEM column. Images of NP samples were recorded on an UltraScan 1000 CCD camera (Gatan, Pleasanton, CA, US).

Cell Culture

The mouse endothelial cell line bEnd.3 (ATCC no. CRL-2299) and HeLa cells (ATCC no. CCL-2) were cultured in DMEM medium (Thermo Fisher Scientific, Waltham, MA, US) supplemented with 10% of fetal bovine serum (FBS) and 1% penicillin-streptomycin. MM.1S (ATCC no. CRL-2974) cells were cultured in RPMI 1640 medium (Thermo Fisher Scientific) supplemented with 10% FBS and 1% penicillin-streptomycin. All cell lines were grown at 37 °C under a 5% CO_2 humidified atmosphere until confluence.

ES Silencing

To investigate ES silencing efficiency, bEnd.3 cells were plated in 24 well plates (150,000 cells per well) and incubated for 24 h prior to endothelial activation with TNF-α (10 ng/mL) for 4 h, following treatment with siControl-NPs or siES-NPs. A serial dilution of each siRNA NP formulation in PBS was prepared at concentrations of 1–60 nM of siRNA. Samples were then incubated for 24 h prior to gene expression analysis. Cells were washed with PBS and harvested using 0.25% trypsin. Cells were disrupted and resuspended in TRIzol™ (Thermo Fisher Scientific, Waltham, MA, US) and RNA was extracted following the manufacturer's protocol. Briefly, 2 µg of RNA was DNAse treated using in a 10 µL reaction containing 1 U/µL RQ1 DNAse, 1× RQ1 DNAse buffer, and 20 U/µL RNAse inhibitor for 30 min at 37 °C and stopped with the addition of 1 µL STOP solution followed by a 10-min incubation at 65 °C. One microliter Oligo dT was added to each reaction and denatured for 5 min at 70 °C and moved immediately to ice. Reverse transcription of the DNAse-treated RNA was carried out in a 20 µL reaction using 1 µL GoScript Reverse Transcriptase (Promega, Madison, WI, US) containing a final concentration of 1× GoScript Reaction Buffer, 2.5 mM $MgCl_2$, 0.5 mM dNTPs using the following cycling: 25 °C for 5 min, 42 °C for 1 h, 70 °C for 15 min, 4 °C hold.

NP Efficacy and Safety In Vitro

To determine efficacy and safety of our NPs in vitro, HeLa cells were plated in 96-well plates (10,000 cells/mL) and treated either with siControl-NPs, siLuc-NPs, or DharmaFECT followed by a 24-h incubation. Twenty-four hours after, either a Luciferase Assay System (Promega, Madison, WI, US) or a CellTiter-Glo Luminescence Cell Viability Assay (Promega) were carried out using a microplate reader to determine siRNA transfection efficiency and toxicity, respectively, following the manufacturer's protocol. All quantifications were done by normalizing experimental groups to the untreated cells group.

Transendothelial Migration Assays

To perform the migration assay, a CytoSelect™ Tumor Transendothelial Migration Assay (Cell Biolabs, Inc., San Diego, CA, US, Catalog No. CBA-216) was used following the manufacturer's instructions. Briefly, each insert was seeded with 1×10^5 bEnd.3 cells in 24-well plates containing culture medium (DMEM supplemented with 10% FBS and 1% penicillin-streptomycin) for 48 h, prior to activation with TNF-α (10 ng/mL) for 4 h, following treatment with siControl-NPs or siES-NPs. Luc+/GFP+MM.1S cells were labeled with CytoTracker and then added to the corresponding inserts. After 24 h of incubation, cells were lysed and mixtures were transferred to a 96-well plate for fluorescence readout at 480 nm/520 nm using a plate reader. Migration data were normalized using data obtained with medium alone. Results are mean ± standard deviation for triplicate assays.

Cell Adhesion Assays

To investigate cell adhesion, bEnd.3 cells were plated in 8-well chambers (ibidi GmbH, Munich, Germany) or 96-well plates (15,000 cells/mL per well) and incubated for 48–72 h prior to TNF-α (10 ng/mL) treatment for 4 h. Further, MM.1S cells (35,000 cells/mL per well) were added on top of bEnd.3 monolayers 24 h after these were treated with siControl-NPs (60 nM) or siES-NPs (60 nM). Monolayers were stained with phalloidin (red) and DAPI (blue) for easier GFP + MM.1S identification, and fixed with 4% (wt/vol) paraformaldehyde (PFA) prior to imaging. The adhesion of Luc+/GFP+MM.1S cells was determined after co-culture with bEnd.3 cells and treatment as described above, using confocal microscopy.

Animal Studies

All animal procedures conducted at the University of Pennsylvania were approved by the Institutional Animal Care and Use Committees (IACUC), and were in accordance with local, state, and federal regulations. For the in vivo studies, female Nod/SCID mice were intravenously (I.V.) injected with Luc+/GFP+MM.1S cells and were randomly divided into four groups after 30 days (n = 10). After injecting MM.1S cells, on day 30 mice were treated with the following: (i) PBS, (ii) free drug (bortezomib), (iii) siES + siCyPA-NPs, and (iv) siES + siCyPA-NPs and bortezomib. Mice were injected intraperitoneal (I.P.) twice a week with 0.5 mg/kg bortezomib or via I.V. injection of siES + siCyPA-NPs (1.0 mg/kg). Mice were sacrificed when they had hindlimb paralysis, cachexia, weight loss of > 15%, or become moribund. Survival data of mice with MM.1S tumors following treatment was assessed.

Statistics

All analyses were performed using GraphPad Prism 9 (La Jolla, CA, US) software; specifically statistical analyses were carried out with unpaired 2-tail t-test unless otherwise stated. Data were plotted as mean ± standard deviation.

Supplementary Information The online version contains supplementary material available at https://doi.org/10.1007/s12195-023-00774-y.

Acknowledgments C.G.F.-E. was supported by a National Science Foundation (NSF) Graduate Research Fellowship (DGE 1845298), a Graduate Education for Minorities (GEM) Fellowship, a University of Pennsylvania's Fontaine Fellowship, and the Hispanic Scholarship Fund (HSF). P. P. G. G. was supported by S. Leslie Misrock Cancer Nanotechnology Postdoctoral Fellowship. R.S.R. was supported by a National Institutes of Health (NIH) T32 multidisciplinary training grant (T32 HL007954) and an NIH F32 postdoctoral fellowship (F32CA243475). M.J.M. acknowledges support from a Burroughs Wellcome Fund Career Award at the Scientific Interface (CASI), a US NIH Director's New Innovator Award (DP2 TR002776), grants from the American Cancer Society (RSG-22-122-01-ET and 129784-IRG-16-188-38-IRG), and a 2018 AACR-Bayer Innovation and Discovery Grant (18-80-44-MITC). The content is solely the responsibility of the authors and does not necessarily represent the official views of the NIH.

Author Contributions CGF-E, PPGG and MJM conceived the project. CGF-E, PPGG, and MJM designed the experiments with input from RSR, LX, and KW. The experiments were carried out by CGF-E and PPGG, and findings were interpreted by all authors. CGF-E and MJM wrote the manuscript. CGF-E prepared figures with input from all authors. All authors edited the manuscript and figures and approved the final version for submission.

Declarations

Conflict of interest C.G.F.-E., P.P.G.G., R.S.R., L.X., K.W., and M.J.M. declare no competing financial interest.

Research Involving Human and Animal Rights All animal procedures conducted at the University of Pennsylvania were approved by the Institutional Animal Care and Use Committees and were in accordance with local, state, and federal regulations. No human studies were carried out by the authors for this article.

References

1. Mahindra, A., T. Hideshima, and K. C. Anderson. Multiple myeloma: biology of the disease. *Blood Rev.* 24:S5–S11, 2010.
2. Kumar, S. K., V. Rajkumar, R. A. Kyle, M. van Duin, P. Sonneveld, M. V. Mateos, F. Gay, and K. C. Anderson. Multiple myeloma. *Nat. Rev. Dis. Primers*. 3:1–20, 2017.
3. Palumbo, A., and K. Anderson. Multiple myeloma. *N. Engl. J. Med.* 364:1046–1060, 2011.
4. Anderson, K. C. Progress and paradigms in multiple myeloma. *Clin. Cancer Res.* 22:5419–5427, 2016.
5. Hulin, C., J. de la Rubia, M. A. Dimopoulos, E. Terpos, E. Katodritou, V. Hungria, H. de Samblanx, A. M. Stoppa, J. Aagesen, D. Sargin, A. Sioni, A. Belch, J. Diels, R. A. Olie, D. Robinson, A. Potamianou, H. van de Velde, and M. Delforge.

Bortezomib retreatment for relapsed and refractory multiple myeloma in real-world clinical practice. *Health Sci. Rep.* 2(1):e104, 2019.
6. Pinto, V., R. Bergantim, H. R. Caires, H. Seca, J. E. Guimarães, and M. H. Vasconcelos. Multiple myeloma: available therapies and causes of drug resistance. *Cancers (Basel)*. 12:1–32, 2020.
7. Krishnan, S. R., R. Jaiswal, R. D. Brown, F. Luk, and M. Bebawy. Multiple myeloma and persistence of drug resistance in the age of novel drugs (Review). *Int. J. Oncol.* 49:33–50, 2016.
8. Robak, P., I. Drozdz, J. Szemraj, and T. Robak. Drug resistance in multiple myeloma. *Cancer Treat. Rev.* 70:199–208, 2018.
9. Ria, R., and A. Vacca. Bone marrow stromal cells-induced drug resistance in multiple myeloma. *Int. J. Mol. Sci.* 21(2):613, 2020.
10. Tang, J., L. Ji, Y. Wang, Y. Huang, H. Yin, Y. He, J. Liu, X. Miao, Y. Wu, X. Xu, S. He, and C. Cheng. Cell adhesion down-regulates the expression of vacuolar protein sorting 4B (VPS4B) and contributes to drug resistance in multiple myeloma cells. *Int. J. Hematol.* 102:25–34, 2015.
11. Niewerth, D., G. Jansen, Y. G. Assaraf, S. Zweegman, G. J. L. Kaspers, and J. Cloos. Molecular basis of resistance to proteasome inhibitors in hematological malignancies. *Drug Resist. Upd.* 18:18–35, 2015.
12. de Bruyne, E., E. Menu, E. van Valckenborgh, H. de Raeve, B. van Camp, I. van Riet, and K. Vanderkerken. Myeloma cells and their Interactions with the bone marrow endothelial cells. *Curr. Immunol. Rev.* 3:41–55, 2007.
13. Vacca, A., R. Ria, F. Semeraro, F. Merchionne, M. Coluccia, A. Boccarelli, C. Scavelli, B. Nico, A. Gernone, F. Battelli, A. Tabilio, D. Guidolin, M. T. Petrucci, D. Ribatti, and F. Dammacco. Endothelial cells in the bone marrow of patients with multiple myeloma. *Blood*. 102:3340–3348, 2003.
14. Roccaro, A. M., T. Hideshima, N. Raje, S. Kumar, K. Ishitsuka, H. Yasui, N. Shiraishi, D. Ribatti, B. Nico, A. Vacca, F. Dammacco, P. G. Richardson, and K. C. Anderson. Bortezomib mediates antiangiogenesis in multiple myeloma via direct and indirect effects on endothelial cells. *Cancer Res.* 66:184–191, 2006.
15. Zhu, D., Z. Wang, J. J. Zhao, T. Calimeri, J. Meng, T. Hideshima, M. Fulciniti, Y. Kang, S. B. Ficarro, Y. T. Tai, Z. Hunter, D. McMilin, H. Tong, C. S. Mitsiades, C. J. Wu, S. P. Treon, D. M. Dorfman, G. Pinkus, N. C. Munshi, P. Tassone, J. A. Marto, K. C. Anderson, and R. D. Carrasco. The cyclophilin A-CD147 complex promotes the proliferation and homing of multiple myeloma cells. *Nat. Med.* 21:572–580, 2015.
16. Winkler, I. G., V. Barbier, B. Nowlan, R. N. Jacobsen, C. E. Forristal, J. T. Patton, J. L. Magnani, and J. P. Lévesque. Vascular niche E-selectin regulates hematopoietic stem cell dormancy, self renewal and chemoresistance. *Nat. Med.* 18:1651–1657, 2012.
17. Natoni, A., T. A. G. Smith, N. Keane, C. McEllistrim, C. Connolly, A. Jha, M. Andrulis, E. Ellert, M. S. Raab, S. V. Glavey, L. Kirkham-McCarthy, S. K. Kumar, S. C. Locatelli-Hoops, I. Oliva, W. E. Fogler, J. L. Magnani, and M. E. Odwyer. E-selectin ligands recognised by HECA452 induce drug resistance in myeloma, which is overcome by the E-selectin antagonist, GMI-1271. *Leukemia*. 31:2642–2651, 2017. https://doi.org/10.1038/leu.2017.123.
18. Barthel, S. R., J. D. Gavino, L. Descheny, and C. J. Dimitroff. Targeting selectins and selectin ligands in inflammation and cancer. *Expert Opin. Ther. Targets*. 11:1473–1491, 2007.
19. Muz, B., A. Abdelghafer, M. Markovic, J. Yavner, A. Melam, N. N. Salama, and ak Azab. Targeting E-selectin to tackle cancer using uproleselan. *Cancers*. 13(2):335–336, 2021.
20. Natoni, A., M. Moschetta, S. Glavey, P. Wu, G. J. Morgan, L. Joshi, J. L. Magnani, I. M. Ghobrial, and M. E. O'Dwyer. Multiple myeloma cells express functional E-Selectin ligands which can be inhibited both in-vitro and in-vivo leading to prolongation of survival in a murine transplant model. *Blood*. 124(21):4718, 2014. https://doi.org/10.1182/blood.V124.21.4718.4718.
21. Nigro, P., G. Pompilio, and M. C. Capogrossi. Cyclophilin A: a key player for human disease. *Cell Death Dis.* 4:e888, 2013.
22. Wang, T., S. Shigdar, H. Al Shamaileh, M. P. Gantier, W. Yin, D. Xiang, L. Wang, S. F. Zhou, Y. Hou, P. Wang, W. Zhang, C. Pu, and W. Duan. Challenges and opportunities for siRNA-based cancer treatment. *Cancer Lett.* 387:77–83, 2017.
23. Chen, D., K. T. Love, Y. Chen, A. A. Eltoukhy, C. Kastrup, G. Sahay, A. Jeon, Y. Dong, K. A. Whitehead, and D. G. Anderson. Rapid discovery of potent siRNA-containing lipid nanoparticles enabled by controlled microfluidic formulation. *J. Am. Chem. Soc.* 134:6948–6951, 2012.
24. Riley, R. S., C. H. June, R. Langer, and M. J. Mitchell. Delivery technologies for cancer immunotherapy. *Nat. Rev. Drug Discov.* 18:175–196, 2019.
25. Riley, R. S., M. N. Dang, M. M. Billingsley, B. Abraham, L. Gundlach, and E. S. Day. Evaluating the nechanisms of light-triggered siRNA release from nanoshells for temporal control over gene regulation. *Nano Lett.* 18:3565–3570, 2018.
26. Kanasty, R., J. R. Dorkin, A. Vegas, and D. Anderson. Delivery materials for siRNA therapeutics. *Nat. Mater.* 12:967–977, 2013.
27. Whitehead, K. A., R. Langer, and D. G. Anderson. Knocking down barriers: advances in siRNA delivery. *Nat. Rev. Drug Discov.* 8:129–138, 2009.
28. Suzuki, Y., and H. Ishihara. Structure, activity and uptake mechanism of siRNA-lipid nanoparticles with an asymmetric ionizable lipid. *Int. J. Pharm.* 510:350–358, 2016.
29. Polack, F. P., S. J. Thomas, N. Kitchin, J. Absalon, A. Gurtman, S. Lockhart, J. L. Perez, G. Pérez Marc, E. D. Moreira, C. Zerbini, R. Bailey, K. A. Swanson, S. Roychoudhury, K. Koury, P. Li, W. V. Kalina, D. Cooper, R. W. Frenck, L. L. Hammitt, Ö. Türeci, H. Nell, A. Schaefer, S. Ünal, D. B. Tresnan, S. Mather, P. R. Dormitzer, U. Şahin, K. U. Jansen, and W. C. Gruber. Safety and efficacy of the BNT162b2 mRNA COVID-19 Vaccine. *N Engl. J. Med.* 383:2603–2615, 2020.
30. Guimarães, P. P. G., C. G. Figueroa-Espada, R. S. Riley, N. Gong, L. Xue, T. Sewastianik, P. S. Dennis, C. Loebel, A. Chung, S. J. Shepherd, R. M. Haley, A. G. Hamilton, R. El-Mayta, K. Wang, R. Langer, D. G. Anderson, R. D. Carrasco, and M. J. Mitchell. In vivo bone marrow microenvironment siRNA delivery using lipid–polymer nanoparticles for multiple myeloma therapy. *Proc. Natl Acad. Sci. U.S.A.* 2023. https://doi.org/10.1073/pnas.2215711120.
31. Dahlman, J. E., C. Barnes, O. F. Khan, A. Thiriot, S. Jhunjunwala, T. E. Shaw, Y. Xing, H. B. Sager, G. Sahay, L. Speciner, A. Bader, R. L. Bogorad, H. Yin, T. Racie, Y. Dong, S. Jiang, D. Seedorf, A. Dave, K. Singh Sandhu, M. J. Webber, T. Novobrantseva, V. M. Ruda, A. K. R. Lytton-Jean, C. G. Levins, B. Kalish, D. K. Mudge, M. Perez, L. Abezgauz, P. Dutta, L. Smith, K. Charisse, M. W. Kieran, K. Fitzgerald, M. Nahrendorf, D. Danino, R. M. Tuder, U. H. von Andrian, A. Akinc, D. Panigrahy, A. Schroeder, V. Koteliansky, R. Langer, and D. G. Anderson. In vivo endothelial siRNA delivery using polymeric nanoparticles with low molecular weight. *Nat. Nanotechnol.* 9:648–655, 2014.
32. Krohn-Grimberghe, M., M. J. Mitchell, M. J. Schloss, O. F. Khan, G. Courties, P. P. G. Guimaraes, D. Rohde, S. Cremer, P. S. Kowalski, Y. Sun, M. Tan, J. Webster, K. Wang, Y. Iwamoto, S. P. Schmidt, G. R. Wojtkiewicz, R. Nayar, V. Frodermann, M. Hulsmans, A. Chung, F. F. Hoyer, F. K. Swirski, R. Langer, D. G. Anderson, and M. Nahrendorf. Nanoparticle-encapsulated siRNAs for gene silencing in the haematopoietic stem-cell niche. *Nat. Biomed. Eng.* 4:1076–1089, 2020.
33. Sago, C. D., M. P. Lokugamage, F. Z. Islam, B. R. Krupczak, M. Sato, and J. E. Dahlman. Nanoparticles that deliver RNA to bone marrow identified by in vivo directed evolution. *J. Am. Chem. Soc.* 140:17095–17105, 2018.

34. Sago, C. D., M. P. Lokugamage, K. Paunovska, D. A. Vanover, C. M. Monaco, N. N. Shah, M. G. Castro, S. E. Anderson, T. G. Rudoltz, G. N. Lando, P. M. Tiwari, J. L. Kirschman, N. Willett, Y. C. Jang, P. J. Santangelo, A. V. Bryksin, and J. E. Dahlman. High-throughput in vivo screen of functional mRNA delivery identifies nanoparticles for endothelial cell gene editing. *Proc. Natl Acad. Sci. U.S.A.* 115:E9944–E9952, 2018.
35. Guimaraes, P. P. G., R. Zhang, R. Spektor, M. Tan, A. Chung, M. M. Billingsley, R. El-Mayta, R. S. Riley, L. Wang, J. M. Wilson, and M. J. Mitchell. Ionizable lipid nanoparticles encapsulating barcoded mRNA for accelerated in vivo delivery screening. *J. Control. Release*. 316:404–417, 2019.
36. Ball, R. L., K. A. Hajj, J. Vizelman, P. Bajaj, and K. A. Whitehead. Lipid nanoparticle formulations for enhanced co-delivery of siRNA and mRNA. *Nano Lett.* 18:3814–3822, 2018.
37. Butowska, K., X. Han, N. Gong, R. El-Mayta, R. M. Haley, L. Xue, W. Zhong, W. Guo, K. Wang, and M. J. Mitchell. Doxorubicin-conjugated siRNA lipid nanoparticles for combination cancer therapy. *Acta Pharm. Sin. B*. 13:1429–1437, 2022.
38. Larrayoz, M., M. J. Garcia-Barchino, J. Celay, et al. Preclinical models for prediction of immunotherapy outcomes and immune evasion mechanisms in genetically heterogeneous multiple myeloma. *Nat. Med.* 29:632–645, 2023. https://doi.org/10.1038/s41591-022-02178-3.
39. Billingsley, M. M., N. Singh, P. Ravikumar, R. Zhang, C. H. June, and M. J. Mitchell. Ionizable lipid nanoparticle-mediated mRNA delivery for human CAR T cell engineering. *Nano Lett.* 20:1578–1589, 2020.

Authors and Affiliations

Christian G. Figueroa-Espada[1] · Pedro P. G. Guimarães[2] · Rachel S. Riley[3] · Lulu Xue[1] · Karin Wang[4] · Michael J. Mitchell[1,5,6,7,8,9,10]

✉ Michael J. Mitchell
mjmitch@seas.upenn.edu

1 Department of Bioengineering, School of Engineering and Applied Science, University of Pennsylvania, 240 Skirkanich Hall, 210 South 33rd Street, Philadelphia, PA 19104, USA

2 Department of Physiology and Biophysics, Institute of Biological Sciences, Universidade Federal de Minas Gerais, Belo Horizonte, MG, Brazil

3 Department of Biomedical Engineering, Rowan University, 201 Mullica Hill Road, Glassboro, NJ 08028, USA

4 Department of Bioengineering, Temple University, Philadelphia, PA 19122, USA

5 Perelman School of Medicine, Abramson Cancer Center, University of Pennsylvania, Philadelphia, PA 19104, USA

6 Perelman School of Medicine, Institute for Immunology, University of Pennsylvania, Philadelphia, PA 19104, USA

7 Perelman School of Medicine, Cardiovascular Institute, University of Pennsylvania, Philadelphia, PA 19104, USA

8 Perelman School of Medicine, Institute for Regenerative Medicine, University of Pennsylvania, Philadelphia, PA 19104, USA

9 Perelman School of Medicine, Penn Institute for RNA Innovation, University of Pennsylvania, Philadelphia, PA 19104, USA

10 Perelman School of Medicine, Center for Cellular Immunotherapies, University of Pennsylvania, Philadelphia, PA 19104, USA